Supplementary Material (ESI) for Lab on a Chip

ELECTRONIC SUPPLEMENTARY INFORMATION (ESI)

High-density micro-arrays for mass spectrometry

Pawel L. Urban,[a] Konstantins Jefimovs,[b] Andrea Amantonico,[a]
Stephan R. Fagerer,[a] Thomas Schmid,[a] Stefanie Mädler,[a]
Josep Puigmarti-Luis,[a] Nils Goedecke,[c] and Renato Zenobi*[a]

[a] *Department of Chemistry and Applied Biosciences, ETH Zurich;*
CH-8093 Zurich, Switzerland
[b] *Laboratory for Electronics/Metrology/Reliability, EMPA, Swiss Federal Laboratories for Material Science and Technology;*
CH-8600 Dübendorf, Switzerland
[c] *Department of Biosystems Science and Engineering, ETH Zurich;*
CH-4058 Basel, Switzerland

* Corresponding author: Prof. Renato Zenobi
Tel: +41 44 6324377
Fax: +41 44 6321292
E-mail: zenobi@org.chem.ethz.ch

Supplementary videos

Movie 1: Water is pipetted onto the non-transparent MAMS with recipient sites 100 μm. When the droplet is drawn back with the pipette, one can observe adhesion of the liquid to the recipient sites and its removal from the adjacent coated area. Following removal of the droplet, the residue water inside the recipient sites dries out within seconds; a slight change in the intensity of the light reflected in the recipient sites can be noticed.

Movie 2: One of the recipient sites of a non-transparent MAMS (100 μm) containing a live cell (*Euglena gracilis*) that constantly swims inside the droplet of liquid medium. High air humidity is maintained to prevent evaporation of the medium and enable observations under microscope.

Experimental details

Materials

Acetone for residual analysis, 9-aminoacridine (9-AA), trifluoroacetic acid (TFA) and Verapamil were purchased from Acros Organics (Geel, Belgium); acetonitrile, adenosine 5'-triphosphate disodium salt (ATP), bovine serum albumin, bradykinin acetate, α-cyano-4-hydroxycinnamic acid (CHCA), guanosine 5'-triphosphate sodium salt (GTP), indium tin oxide (ITO)-coated glass slides, 1-(3-*sn*-phosphatidyl)-*rac*-glycerol sodium salt, sinapinic acid and uridine 5'-diphosphoglucose disodium salt (UDP-Glucose) from Sigma-Aldrich (Buchs, Switzerland); angiotensin II acetate from Bachem (Bubendorf, Switzerland); ethanol from Scharlab (Sentmenat, Spain); 1H,1H,2H,2H-perfluorooctyldimethylchlorosilane from ABCR (Karlsruhe, Germany); and 1H,1H,2H,2H-perfluorododecane-1-thiol from Asemblon (Redmond, WA, USA). Standard solutions were usually prepared using LC-MS grade water (Sigma-Aldrich).

CHCA and sinapinic acid matrices were prepared by dissolving 10.0 mg of a chemical with 1 mL of 1:1 (v/v) mixture of water and acetonitrile and adding 1 μL of TFA. The 9-AA solution was prepared by dissolving 9.0 mg of 9-AA in 1 mL of acetone. For matrix application by ultrasound-assisted spray, the 9-AA solution was diluted 1:1 (v/v) with acetone; then, 50-100 μL of water was added per 1 mL of the resulting 4.5 mg mL^{-1} 9-AA solution.

The cultures of *Euglena gracilis*, *Tetrahymena pyriformis* and *Cosmarium turpinii* were obtained from Carolina Biological Supply Company (Burlington, NC, USA). The culture of *Chlamydomonas reinhardtii* expressing green fluorescent protein (GFP) (IFT20) was obtained from Mr. Huy Buy (Group of Dr. Takashi Ishikawa, ETH Zurich). Baker's yeast (*Saccharomyces cerevisiae*) were obtained from a local supermarket and incubated with 1% sucrose solution at 30°C prior to experiments. All kinds of cells were concentrated to a desired density before spreading them on MAMS. Typically, 0.5 mL of the original cell culture was mixed with 1.5 mL of cold water and centrifuged for 5 min at 1000 rcf. Then, the pellet was resuspended in 50-100 μL of cold water. The resulting dense suspension of cells was directly applied to MAMS.

Fabrication of MAMS

Various versions of the micro-arrays for mass spectrometry were initially tested: First, we tried using commercial polymeric "nanotiter plates". Second, we attempted printing a hydrophobic pattern of 1H,1H,2H,2H-perfluorooctyldimethylchlorosilane onto glass or ITO-glass with a polydimethylsiloxane (PDMS) stamp with a checkerboard pattern. Third, we patterned gold-coated glass and mica slides using a picosecond laser. Before the ablation, the gold surface had been derivatized with 1H,1H,2H,2H-perfluorododecane-1-thiol, in order to make it hydrophobic as well as "organo-phobic". Among these three initial attempts, only the last one gave a promising result (**Fig. S1**). However, these micro-arrays were easily damaged during cleaning.

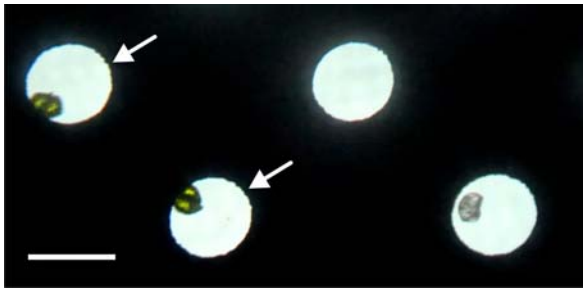

Figure S1. MAMS realized using a transparent support coated with gold. Arrows indicate recipient sites with the cells of *Cosmarium turpinii*. Scale bar: 100 µm.

Eventually, we opted for stainless steel plates, coated with a layer of polysilazane (EpoTec 611/2320; Eposint, Pfyn, Switzerland; coating CAG 37 marketed by Clariant Produkte, Frankfurt am Main, Germany). As demonstrated earlier, laser ablation can be readily used to fabricate sample-focusing plates for MALDI (McLauchlin *et al.*, 2007; Torta *et al.*, 2009). Here, the polysilazane layer coated on a conductive support was structured by picosecond laser ablation. A Nd:YAG-laser (SuperRapid from Lumera Laser, Kaiserslautern, Germany), which delivers ~ 10 ps long pulses, was used with the following parameters: wavelength, 355 nm; repetition rate, 50 kHz; average power, 100 mW. The laser beam was focused and scanned over the surface of the sample using a galvanoscanner (hurrySCAN 10 from Scanlab, Puchheim/Munich, Germany). The telecentric lens with a 100 mm working distance provides a constant focal spot of ~ 10 µm at the surface over the scanned area. The scan speed (150 mm s^{-1}) and the hatch were selected to have a 3 µm spot-to-spot distance. In this way, MAMS with spot diameters from 500 down to ~10 µm could easily be machined. The spacing

between the rows of the ablated sites was usually maintained at 100 μm. In the final stage of the study we worked mainly with 50 and 100 μm MAMS since these dimensions matched the laser beam focus in the MALDI-MS instruments available for this study. Later, we also found that, it is possible to fabricate MAMS in completely transparent conductive supports; this can be achieved by replacement of the metal support with ITO glass slides coated with polysilazane (*cf.* **Fig. 1C**). These transparent MAMS enabled thorough observations of cells (especially small cells, such as yeast, *Saccharomyces cerevisiae*) with inverted microscope. Unlike the early version with the gold layer (**Fig. S1**), the MAMS made of ITO glass were quite robust and the surface did not deteriorate when cleaning with ethanol and during sonication.

Scanning electron microscopy (SEM) and atomic force microscopy (AFM) were used to examine surfaces of the polysilazane-coated stainless-steel MAMS before and after ablation with the picosecond laser (**Figs. S2** and **S3**). Clearly, even a single ablation stage completely removes the layer of polysilazane (**Fig. S2A**). Although the ablation process exposes and even increases the microscale roughness of the steel surface, the hydrophilic properties of the bare steel surface are preserved.

When maintaining MAMS in an environment with high humidity, water condensation occurs on the surface and gives rise to formation of small droplets (**Fig. S4**). Condensation at high air humidity leads to the growth of bigger droplets at the recipient sites (the laser-ablated areas) while small droplets cover the area between the recipient sites (*cf.* **Fig. 1C**). Therefore, pieces of the solid material (*e.g.* cells) trapped in the large droplets are separated at all times, even during prolonged microscopic observations at relatively high humidity (maintained to prevent evaporation of the liquid carrier).

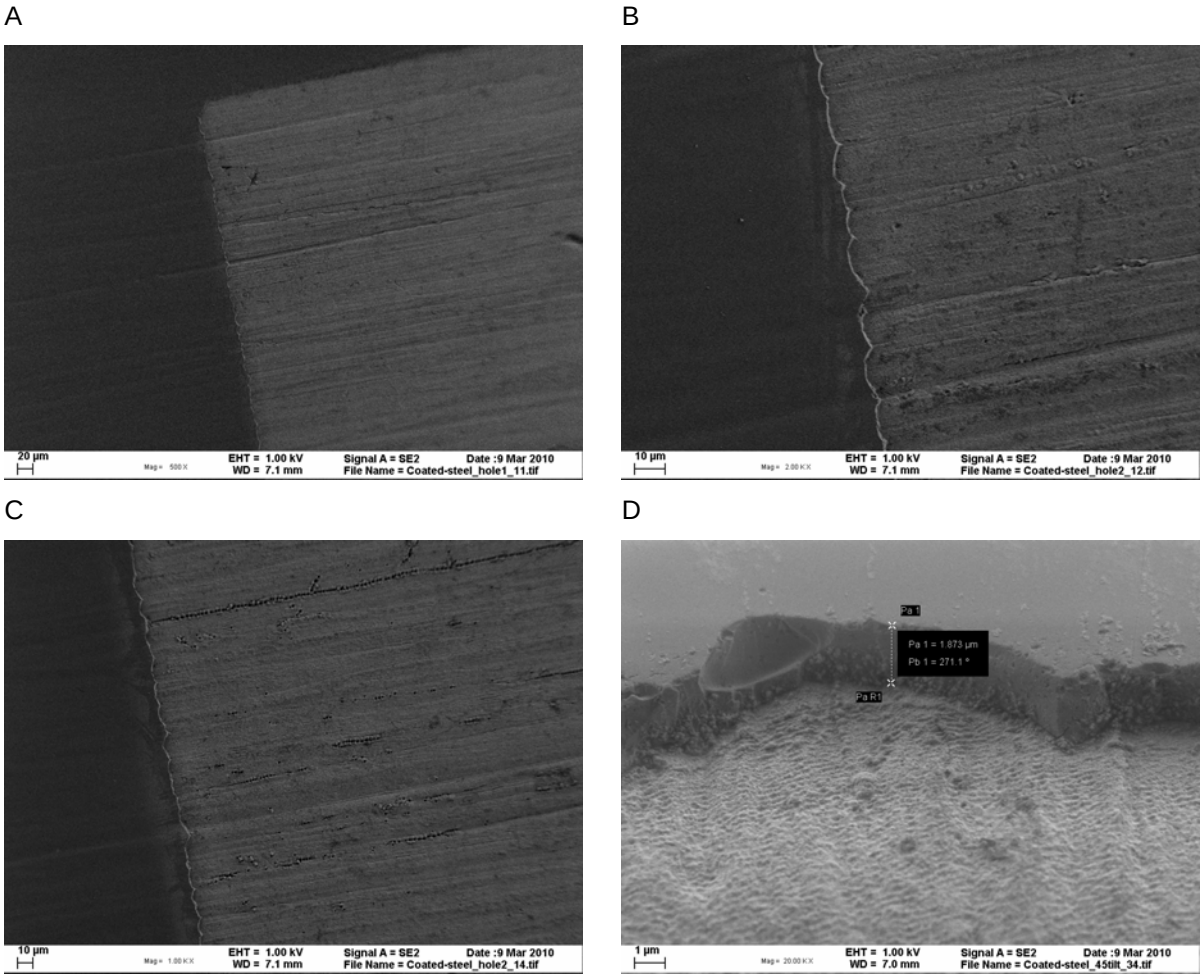

Figure S2. Scanning Electron Microscopy images after ablation of polysilazane-coated stainless steel plate with picosecond-laser. (A) 1×, (B) 2×, (C) 5× laser ablation, (D) SEM of the edge of a recipient site (after fabrication with ps-laser, 5× ablation, SEM tilt 45°): upper part – polysilazane coating, lower part – the ablated area (stainless steel). Coating thickness: ~ 3 µm.

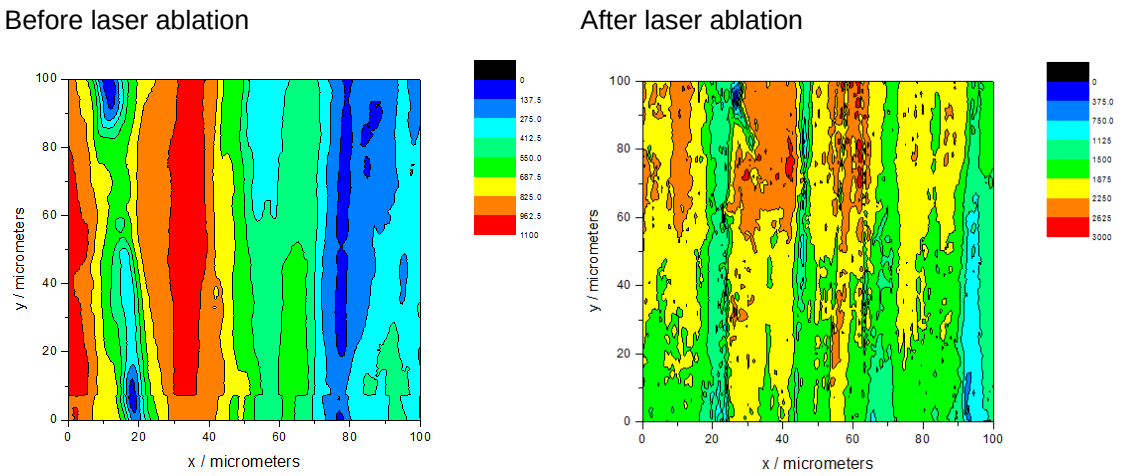

Figure S3. Atomic force microscopy (topography imaging) before (left) and after (right) laser patterning of the micro-array. Vertical scales: 0-1100 (left) and 0-3000 nm (right).

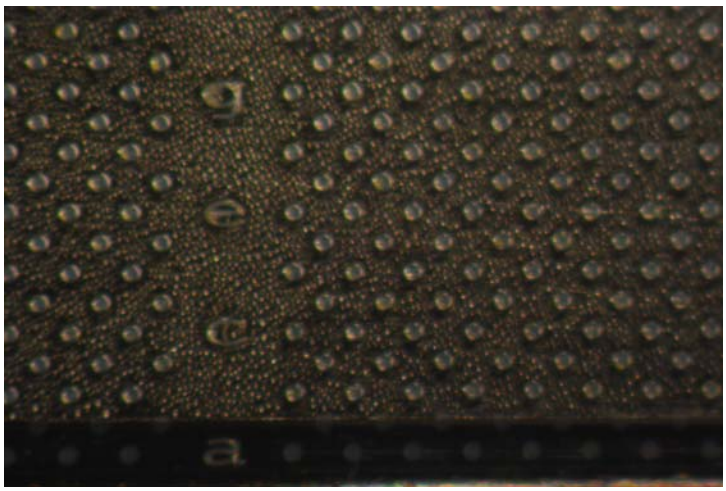

Figure S4. "Large" (picoliter-volume) water droplets in the 100-µm recipient sites of a non-transparent MAMS and water condensation in the area between the recipient sites.

Cell analysis

Cells can easily be distributed in MAMS by pulling a droplet of cell suspension over the microarray surface with a glass slide or piece of plastic (**Fig. S5**). The "checkerboard" pattern of MAMS is preferred to achieve this.

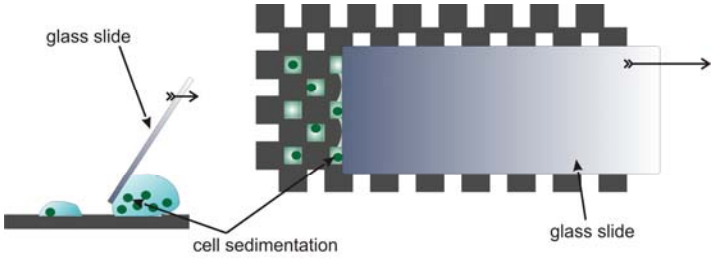

Figure S5. A simplified view of cell deposition on a checkerboard-patterned MAMS.

This section describes an auxiliary (optional) house-built setup implemented to facilitate spreading cell suspensions on MAMS in the present study. It incorporated a box of styrofoam (ca. 32 × 26.5 × 24.5 cm (w/h/d)), used for thermal insulation, **Fig. S6**. A Peltier-based air-air thermoelectric cooler assembly (AA-040-12-22; Minco, Wil, Switzerland) was used for thermostatting; it was connected to a controller (TC2812; CoolTronic, Rossrüti, Switzerland) and a temperature sensor (S458PDZ12; Minco). A simple optical system with a microscope objective (PLAN APO ELWD 10×/0.28 WD-33.5) was integrated in the box for optional monitoring of the cell seeding process. The image was relayed, via a microscope eyepiece (Kpl 16×, Zeiss, Göttingen, Germany), onto a miniature CMOS camera (size: 15 × 22 mm, lens: f=3.6mm, 250K (NTSC)). An ultrasonic terrarium humidifier ("Repti Fogger"; Zoo Med Europa, Ekeren, Belgium) was used to saturate the box with water vapor; a flexible hose was used to direct the fog stream from the ultrasonic generator (outside the styrofoam box) onto the MAMS (inside the box). Another portable ultrasonic nebulizer (specified droplet size: 0.5 to 5 µm, MY-520; Mickeyoo Electrical Appliance Company, Shenzhen, China) was also routinly used to prevent evaporation of sub-nanoliter volumes of liquid samples on the ablated sites with the diameter of 100 µm or smaller, during prolonged observations under microscope. When implementing the transparent MAMS for analysis of smaller unicellular species (*e.g. Saccharomyces cerevisiae*), an inverted microscope was used to monitor seeding and counting of the cells. A humidity chamber has been fitted onto the stage of the microscope. The same humidity generators as those described above were used together with a humidity controller (Humidity Control II; Lucky Reptile, Waldkirch, Germany) to maintain constant humidity (typically, 75%) during microscopic observations.

MALDI matrix (typically, 9-aminoacridine) was applied to the cells deposited on the MAMS using an ultrasound-induced spray (**Fig. S7**), operated under ambient conditions. The

metal tip of an ultrasonic scaler (UDS-J; Woodpecker Medical Instrument Company, Guilin, Guangxi, China) was dipped in a microcentrifuge tube filled with the matrix solution. When spraying, the plate bearing MAMS was moved in front of the opening of the tube. This step requires special safety precautions (*e.g.* work inside fume hood, wear face mask, safety glasses, gloves, lab coat; place the nozzle and the sample in a box wrapped with plastic foil) since some of the MALDI matrices (especially 9-aminoacridine) are toxic. The matrix solution, and the aerosol particles generated by the ultrasonic spray, must not have contact with skin, be ingested or breathed in. When spraying the MAMS with a MALDI matrix solution, attention also needs to be paid to the size of droplets landing on the MAMS surface; large droplets are likely to form bridges between individual recipient sites which usually leads to cross-contamination.

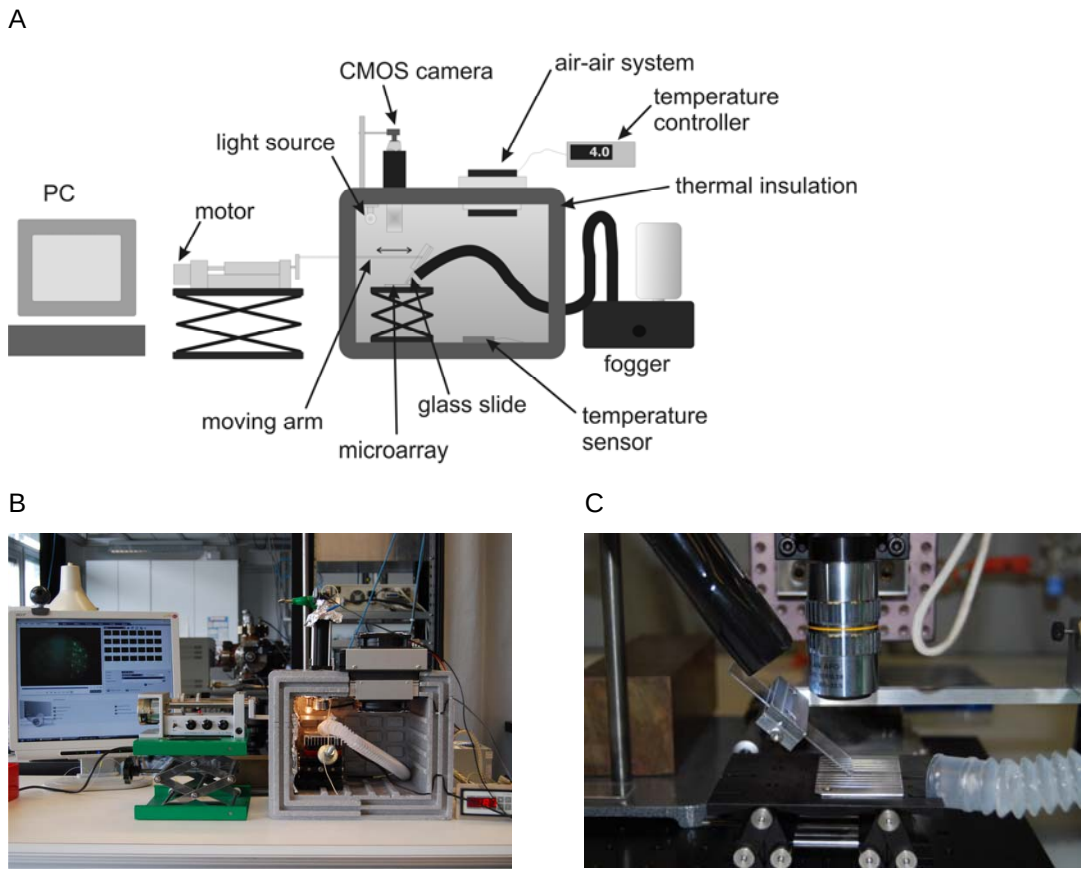

Figure S6. A simple thermostatted system used for deposition of cells on MAMS: (A) schematic, (B) photograph. (C) Early version of the experimental setup used for spreading cell suspensions on the MAMS. The plastic hose delivers highly humid air that prevents evaporation of water droplets from the micro-array recipient sites. This way, cells can stay alive on the MAMS until visual inspection and counting are finished.

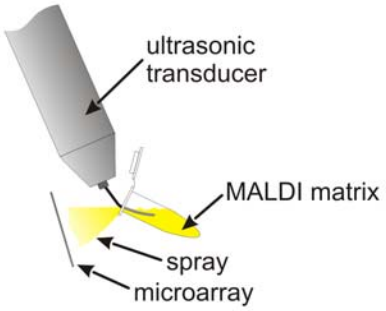

Figure S7. An ultrasonic transducer adapted for spraying the MALDI matrix solution on the surface of MAMS.

Mass spectrometry

Initial work was done using a MALDI-TOF-MS instrument (Axima; Shimadzu/Kratos Analytical, Manchester, UK) equipped with a 337 nm nitrogen laser, **Figs. 2A**, **2B** and **3A**. Later on, MAMS were also used with MALDI-TOF/TOF-MS 4800 *Plus* (AB Sciex, Concord, ON, Canada) equipped with a 355 nm solid-state laser and a high mass detector (HM2 "Tuvo"; CovalX, Zurich-Schlieren, Switzerland), **Figs. 2C** and **4**. Except for the analysis of the high-mass protein, reflectron mode was used.

MAMS are highly compatible with the commercial data acquisition packages (**Fig. S8**); the mass spectra were acquired using the standard programs supplied by the instrument manufacturers: Shimadzu/Kratos Analytical and AB Sciex. A template for automatic scanning of the MAMS surface was created which enables acquisition of 200 spectra corresponding to individual samples (*e.g.* single cells) in 75 s (with 10 laser shots per spectrum). When performing cell analysis by means of the 50 or 100 μm MAMS using the MALDI-MS instrument from Shimadzu/Kratos Analytical, we collected 16 sub-spectra (2 laser shots each). When using the MALDI-MS instrument from AB Sciex, we applied from 10 to 100 laser shots. Laser power used for ionization was optimized separately for each of the MALDI-MS instruments.

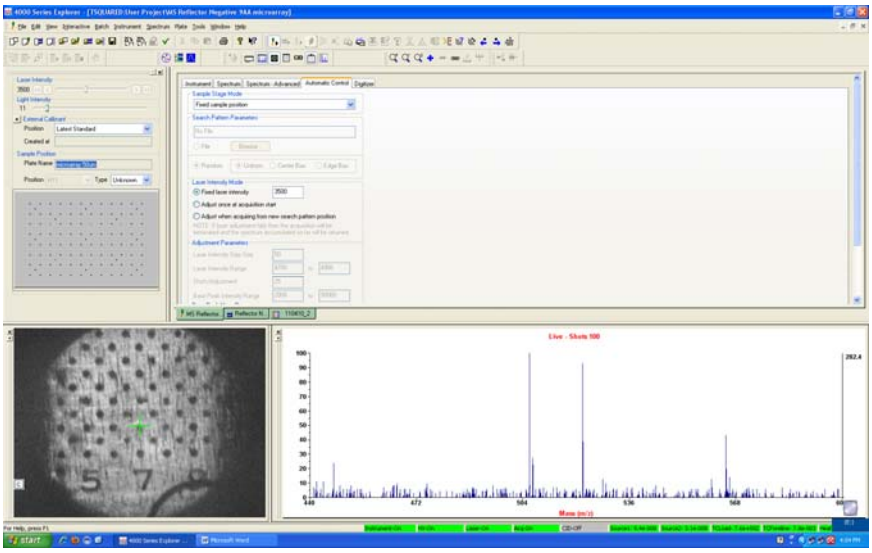

Figure S8. Screen snapshot from a commercial software for data acquisition from the AB Sciex 4800 MALDI-MS instrument; here used to acquire MS spectra from the MAMS with the diameter of individual recipient sites (black spots in the camera view): 50 µm.

Fluorescence and Raman spectroscopy

Fluorescence and Raman microspectroscopic measurements were performed using an upright NTegra SPECTRA system from NT-MDT (Zelenograd/Moscow, Russia). This instrument is equipped with a white-light microscope with CCD camera for optical observation of the sample and a confocal laser microscope. In both cases, light is focused onto the sampled by a 100×/0.7 N.A. objective offering long-working distance and high numerical aperture and light backscattered from the sample as well as fluorescence emission are collected by the same objective. For excitation, a diode-pumped solid-state (DPSS) laser having a wavelength of 532 nm and a HeNe laser at 632.8 nm are coupled to the instrument via fiber optics. A photomultiplier tube (PMT) is employed for detection of the backscattered light and wavelength-shifted light (Raman scattering and fluorescence emission) is guided to a spectrometer with charge-coupled device (CCD) detection (Newton, Andor, Belfast, UK). Optionally, modules for atomic force microscopy (AFM) and scanning tunneling microscopy (STM) can be inserted between objective and sample. Since all different microscopy techniques observe the sample from the top, the system can handle both, transparent and opaque samples. For imaging, the sample or the laser spot can be scanned using piezoelectric actuators. Piezoelectric scanning, change of optics for switching the lasers and choosing the laser power as well as collection of signals are controlled by the software ‘NT-MDT Nova’.

For the measurements described here, a MAMS with *Chlamydomonas reinhardtii* cells was inserted into the instrument without any special sample holder. The spots were found by moving the MAMS using micrometer screws that are integrated into the sample scanning stage and simultaneous observation of the sample surface by using the white-light microscope module offering a field of view of more than 100×100 μm^2. Once a spot with one or more cells was identified, the optical image was collected and the system was switched to laser microscope mode. In this mode, the laser spot was scanned over the sample surface and PMT images (data not shown) as well as full-spectroscopic mappings (with the full Raman or fluorescence spectrum collected at every pixel) were collected. 532-nm laser irradiation was found to yield strong Raman bands of β-carotene due to resonance enhancement, whereas 632.8-nm excitation was employed for measurement of the chlorophyll fluorescence. Both, Raman and fluorescence measurements yielded strong signals in very short collection times. Therefore, it was possible to strongly attenuate the laser power for avoiding sample damage. For both kinds of measurement, laser powers of a few tens of microwatts and measurement times of 30-50 ms were employed in mapping experiments.

Fig. 3B shows the distribution of the fluorescence intensity at the emission maximum of 684 nm in a 32×32-pixel mapping over 12.8×12.8 μm^2. Thus the size of one pixel is 400 nm and the whole mapping experiment took ~30 s. The diffraction-limited optical resolution of the microscope is ~600 nm when using the 632.8-nm laser. For the Raman spectrum shown in **Fig. 3C** a longer collection time of 0.5 s was chosen and the spectrum was accumulated 20 times to improve the signal-to-noise ratio.

Additional results and discussion

MS peak assignment

Identification of most peaks in the single-cell MALDI-MS spectra was straightforward and based on the knowledge of the species that can be ionized by certain matrices (for 9-AA, see Edwards and Kennedy (2005)), and in some cases using MS/MS spectra (see for example, Sun *et al.* (2007)). Identification of the peak at *m/z* 793.5, observed in the spectra of single cells of *Chlamydomonas reinhardtii* (**Fig. 3A**), was conducted based on (i) two independent exact mass measurements using MALDI-TOF-MS and MALDI-TOF/TOF-MS instruments, (ii) exact mass measurement using a MALDI-FTICR-MS instrument, and (iii) MS/MS measurements obtained by CID fragmentation of the parent ion in a MALDI-TOF/TOF-MS instrument (**Fig. S9**).

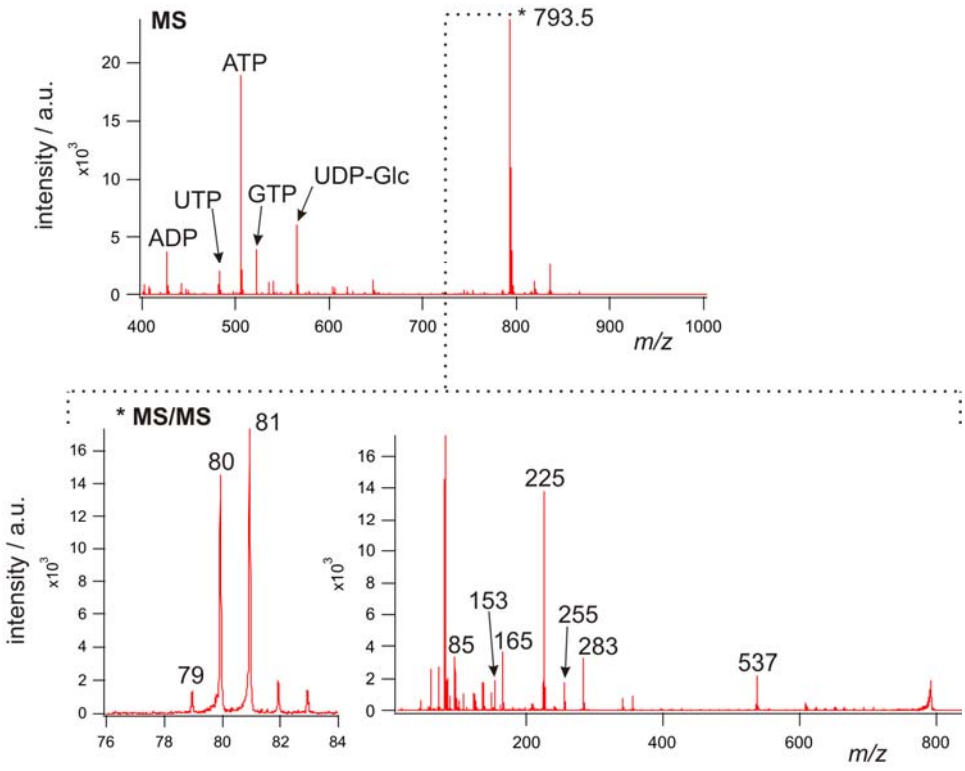

Figure S9. MALDI-MS/MS spectrum of the species at m/z 793.5 observed during analysis of the sample of *Chlamydomonas reinhardtii* mixed with the 9-AA matrix (negative ion mode).

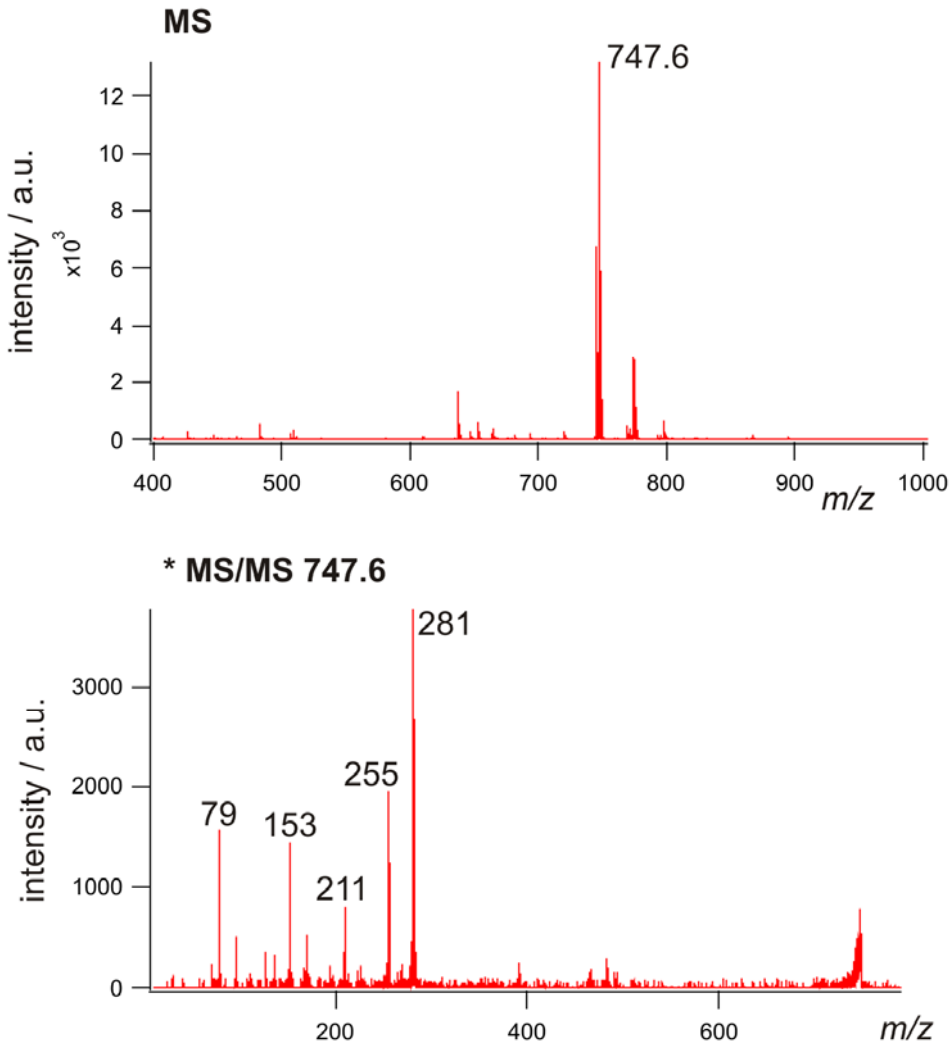

Figure S10. MALDI-MS/MS spectrum of 1-(3-*sn*-phosphatidyl)-*rac*-glycerol (0.1 mg mL^{-1} in ethanol) from Sigma-Aldrich mixed with the 9-AA matrix (negative ion mode).

Samples composed of multiple cells were used for these identification experiments. The measured exact masses were compared with the species listed in the metabolite database at www.hmdb.ca. The MALDI-FTICR-MS measurement yielded a peak at the *m/z* 793.5025 (negative ion mode), which is in excellent agreement with the theoretical monoisotopic mass of 793.50251, predicted for the ion $[C_{44}H_{75}O_{10}P\text{-}H]^-$. The eight best matches in the www.hmdb.ca database (viewed on 5th May 2010) correspond to phosphatidylglycerols with two fatty acids with a total number of 38 carbons and a total number of 6 double bonds. Some of the peaks in MS/MS spectra also support the phosphorylated glycerol core: the fragment at the *m/z* of 153 may correspond to the phosphorylated glycerol after subtraction of one water molecule (*cf.* Gilleron *et al.*, 2006): this is in agreement with an MS/MS spectrum of a

standard phosphatidylglycerol purchased from Sigma-Aldrich (**Fig. S10**). The MS/MS spectrum of the peak at the *m/z* 793.5 observed for the sample of *C. reinhardtii* (**Fig. S9**) was further analyzed using Mass Frontier software (ver. 6.0; HighChem, Bratislava, Slovakia). It was found that depending on the positions of double bonds in fatty acids and the relative lengths of the chains in the hypothetical molecular structure, different peaks in the MS/MS spectrum (**Fig. S9**) could be explained. This suggests that the peak at the *m/z* 793.5 may correspond to a mixture of isomeric ions with the same nominal mass but different molecular structures.

In a similar way, by conducting MS/MS analysis, we attempted to classify other peaks in mass spectra of *Euglena gracilis* spotted with the 9-AA matrix. CID-induced fragmentation of the species represented by several other peaks with *m/z* > 700 was found to yield a phosphate anion (PO_3^-, *m/z* 79). One of them was Acetyl-CoA, the others require further identification.

Comparison with our earlier single-cell MS

A number of chemical species in relatively large cells can be analyzed by MS using bare MALDI plates in a low-throughput fashion. MAMS provide a tool for conducting cell analysis in a high-throughput manner while preserving the high sensitivity of the MALDI-MS method. Since they minimize mechanical stress exerted on the cells, they should be suitable for analysis of primary metabolites.

When cells of *Euglena gracilis* were analyzed by transferring them with a microscale capillary onto a conventional MALDI plate, the MS peaks corresponding to some of the most abundant metabolites (ADP and ATP) appeared to have very low signal-to-noise ratios (**Fig. S11**); when the cells of the same species were analyzed using MAMS, several metabolite ions yielded peaks with *S/N* values above 10 (**Fig. 2B**). This, taken together with the results depicted in **Fig. 4**, shows that MAMS enable analysis of cells smaller than those that could be studied using conventional MALDI supports.

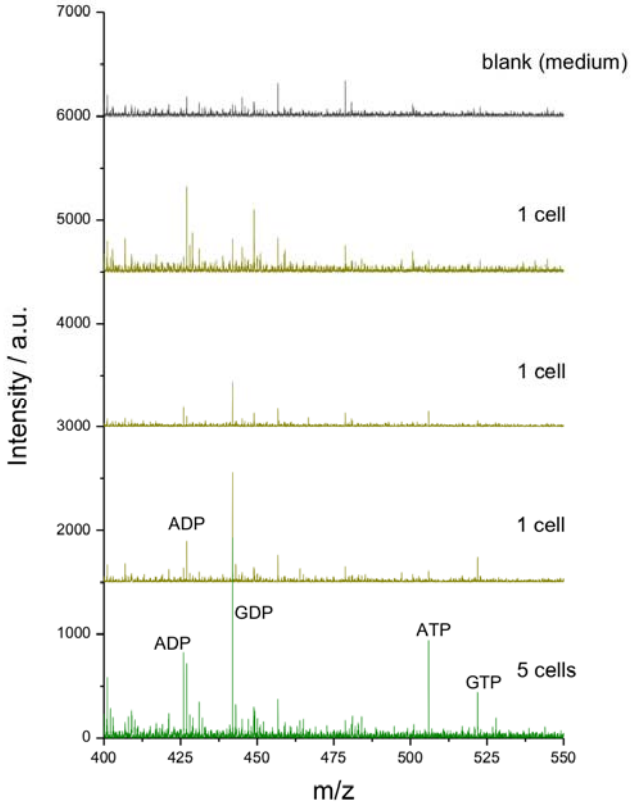

Figure S11. Cells of *Euglena gracilis* analyzed using standard MALDI plates; manual deposition of individual cells (using microscope and a capillary) followed by addition of MALDI matrix (best occurrences). Low *S/N* ratio observed for scarce metabolites detected in individual cells.

An early prototype of MAMS consisted of a micro-array with larger (square) recipient sites than those presented here (**Fig. S12**). Conversely, in the final version of MAMS, the recipient sites were round, and had diameter equal to or smaller than the laser beam focus in the MALDI-MS instrument (**Fig. 2B**), which, according to prior knowledge, provides a sensitivity gain (Amantonico *et al.*, 2008). As a consequence, a high *S/N* for relatively small cells can be achieved. However, using the older version, larger cells of another species – *Cosmarium turpinii* – were spread on the micro-array: they were instantly concentrated in the hydrophilic recipient sites (**Fig. S12**). Then, the microscope observations were carried out (photograph): the cells (green dots) inside the recipient sites (bright squares) were counted. Subsequently, MALDI matrix was applied and the MALDI-MS spectra obtained. It is easy to

see that the peak of an abundant metabolite, adenosine triphosphate, scales directly with the number of cells present in the recipient sites. However, *S/N* ratios are lower than those achieved for even smaller cells using the final version of MAMS (**Figs. 2B-C** and **3A**). It must be mentioned that such a comparison is based on an assumption that concentrations of primary metabolites are comparable in different microbial cells; this assumption is not always accurate.

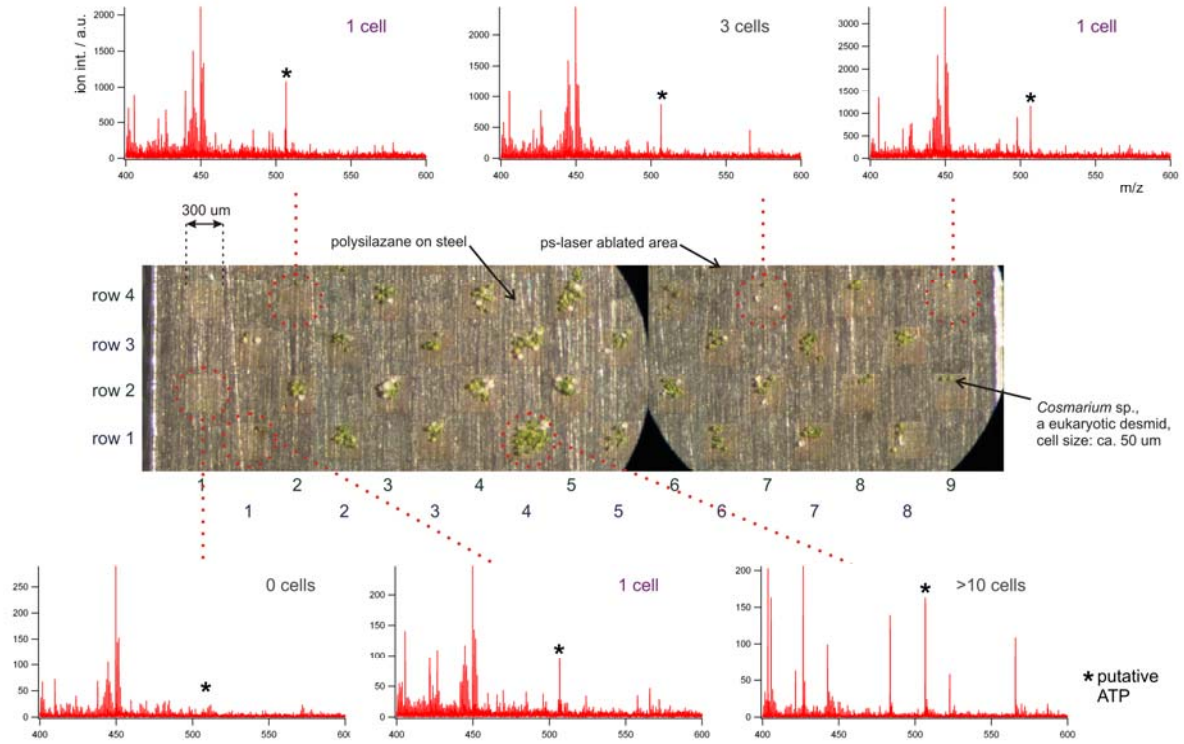

Figure S12. The concept of cell analysis with MAMS, explained here using an early prototype (square recipient sites with a dimension of 300 μm).

Sensitivity

Fig. S13 is an extension of the result depicted in **Fig. 4**. The additional MS spectra, obtained for greater analyte concentrations, show that the signal-to-noise ratios scale with the amounts of analytes present in the recipient sites. Referring to the result depicted in **Fig. 4D** (**S13D**), it should be pointed out that, from our experience, the sensitivity of the high-mass detector for bovine serum albumine is about 2× greater than that observed when using standard microchannel plate detector.

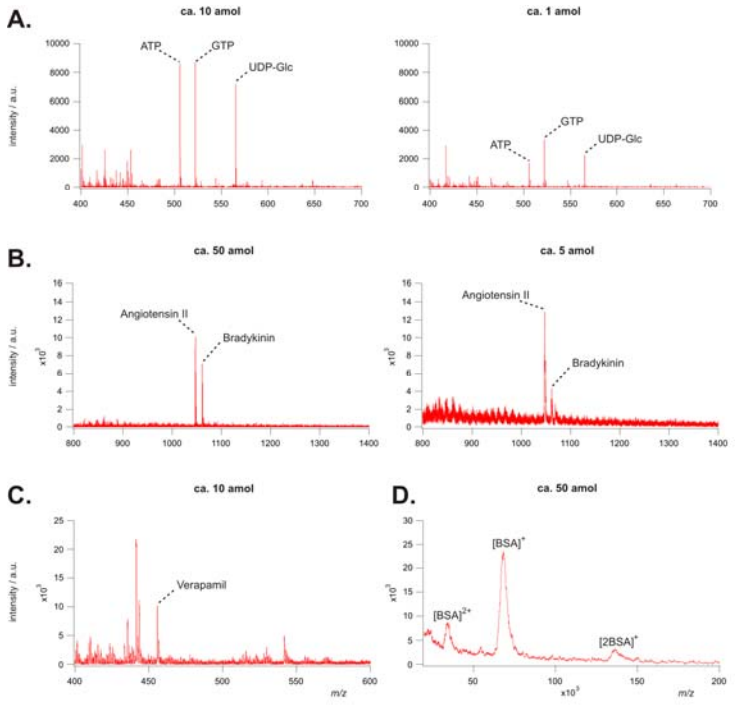

Figure S13. Extended version of **Fig. 4** from the main text. Low-attomole-level sensitivity observed for a variety of analytes using the 50 µm MAMS: (A) three primary metabolites (ATP, GTP and UDP-Glc; negative ion mode; matrix: 9-aminoacridine), (B) two peptides (angiotensin II and bradykinin; positive ion mode; matrix: α-cyano-4-hydroxycinnamic acid (CHCA)), (C) Verapamil (positive ion mode; matrix: CHCA), (D) bovine serum albumine (BSA; positive ion mode with high mass detector; exponential smoothing; matrix: sinapinic acid). MALDI-MS instrument: AB Sciex 4800.

In order to calculate the approximate amounts of analytes loaded into the individual recipient sites, one needs to estimate the volume of the sample left on the micro-array after sweeping the MAMS with sample (*cf.* **Fig. 1A** and **Movie 1**). For estimation of the droplet volumes we initially assumed that the droplet has a shape as shown in **Fig. S14A**. Microscopic observations of droplets on MAMS with recipient sites 50 µm (**Fig. S14B**) and 100 µm (**Fig. S14C**) confirm this assumption. However, one cannot exclude that the calculation shown in **Fig. S14A** slightly overestimates the droplet volume for the 50 µm MAMS, leading to small overestimation of the reported limits of detection. Thus, the real limits of detections might be even lower than those indicated in this article.

In **Movie 1**, almost all droplets evaporate. One droplet is an artefact due to the manual pipetting; it has a considerably larger volume than all other droplets.

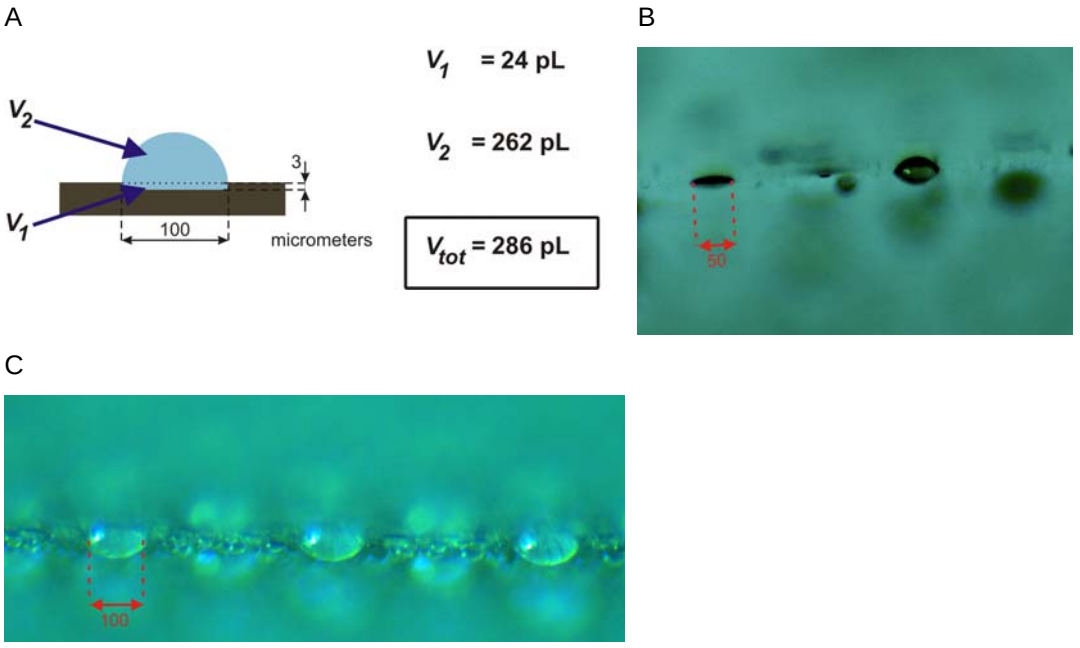

Figure S14. (A) Calculation of the droplet volume (example) inside a recipient site with diameter of 100 µm. Water droplets on MAMS: (B) 50 µm, (C) 100 µm. Microscope pictures taken from a sharp angle. Water was dispensed with a pipette (*cf.* **Fig. 1A**). High humidity was maintained during microscopic observations to prevent instantaneous evaporation of droplets. The shapes of the water droplets suggest that they have a hemispherical shape, similar to the one approximately sketched in (A).

When using the "push & pull" method for deposition of samples with a pipette, it is possible to leave on the MAMS surface only the tiny amount of liquid that adheres to the wettable recipient sites. This amount of sample is sufficient for the MS analysis. Almost no sample is left in the area between the recipient sites. The remainder is pulled back and stays in the pipette tip, and it can be kept for analysis using other methods. Moreover, using MAMS, it is not necessary to scan the sample deposit for "sweet spots", as in conventional MALDI-MS analysis, because the whole sample is irradiated. Since each recipient site on MAMS contains a limited amount of ionizable species, after several shots of the UV laser in the MALDI mass spectrometer, the residual analyte available for ionization will be significantly lower than at the beginning of the analysis. This is clearly illustrated in **Fig. S15**. The ability to involve the whole amount of the sample in the MALDI process should enable analyte quantification based on integration of the MS signals from all the sub-spectra acquired during analysis, until the last one in which any analyte peak above the LOD threshold appears.

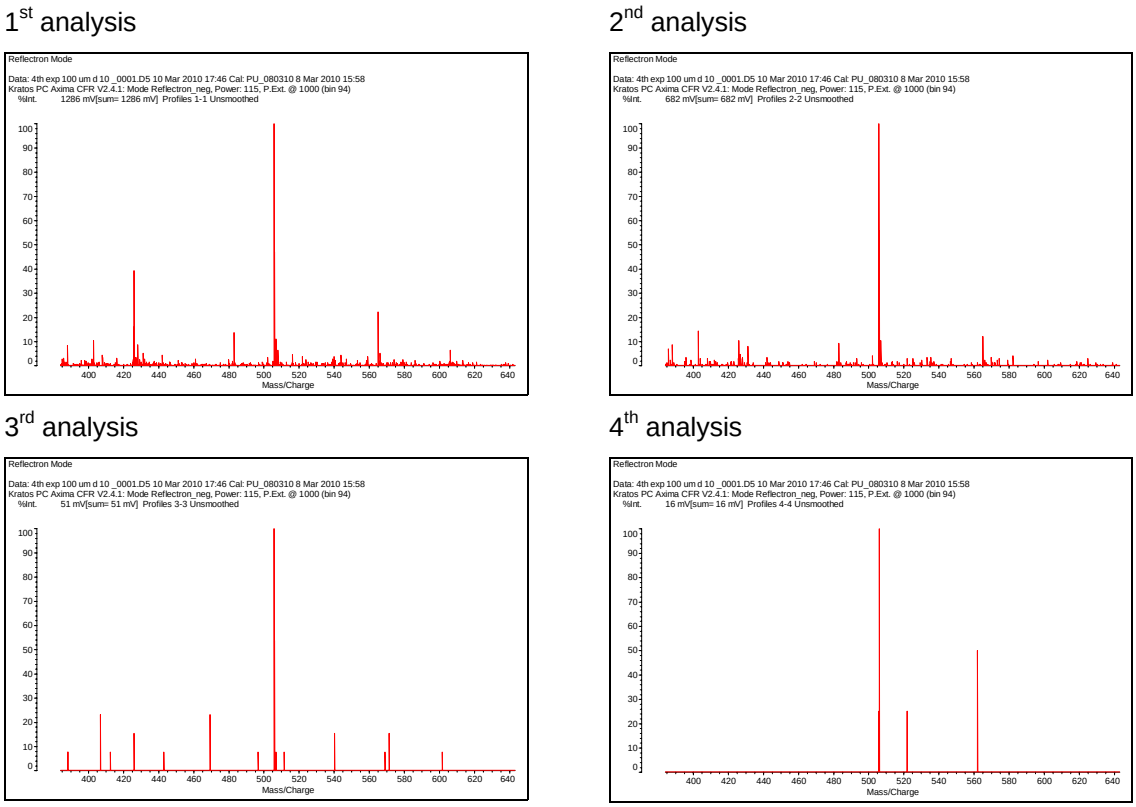

Figure S15. Signal decay due to depletion of the analytes by UV laser irradiation in the MALDI-MS instrument. In this case, one recipient site of MAMS was irradiated several times (5 laser shots each time). The *S/N* ratio decreases which indicates depletion of the analyte. The most prominent peak corresponds to ATP.

Assignment of Raman bands

As shown in **Fig. S16**, all Raman bands in the spectrum of *Chlamydomonas reinhardtii* collected with a laser wavelength of 532 nm can be assigned to β-carotene. As known from the literature (see for example Saito *et al.* (1983)), the most prominent bands at 1154 cm^{-1} and 1520 cm^{-1} are due to C-C and C=C stretching vibrations of the conjugated double bond chain. For confirmation, a reference spectrum of pure β-carotene powder (Fluka) was collected using the same instrument with the same excitation wavelength. As can be seen, the band positions exactly match the Raman signals of *C. reinhardtii*. Our spectra are in good agreement with those obtained by Kubo *et al.* (2000). The bands at > 2000 cm^{-1} can be assigned to overtones and combinations of the bands in the range of 1002-1520 cm^{-1}. The band at 2164 cm^{-1} can be interpreted as combination of the modes at 1002 cm^{-1} and 1154 cm^{-1}. The band at 2308 cm^{-1} is the first overtone of the mode at 1154 cm^{-1}. These two bands are overwhelmed by

fluorescence in the *C. reinhardtii* spectrum, most likely the rising edge of the chlorophyll fluorescence emission.

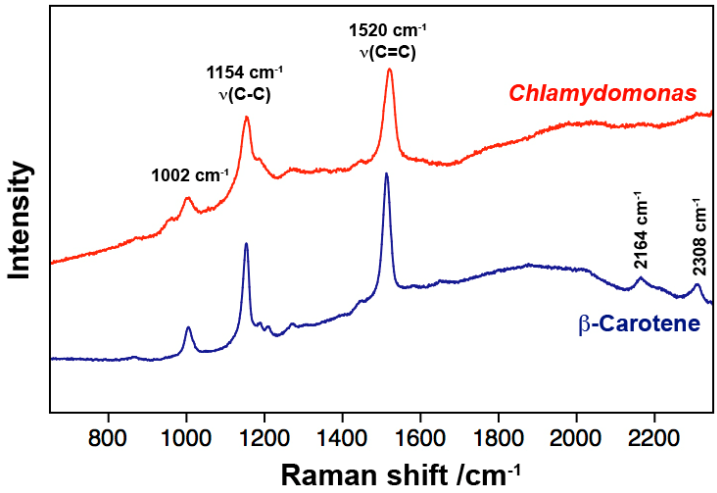

Figure S16. Raman spectrum (λ = 532 nm) of *Chlamydomonas reinhardtii* (extension of **Fig. 3C**) compared to a reference spectrum of β-carotene powder.

Multiple detection with MAMS

As explained in the main text, MAMS with labeled sample spots offers the possibility to study the same spot with complementary techniques. In addition to MALDI-MS, we demonstrate the feasibility to study cells on MAMS by optical, fluorescence and Raman microscopy. **Fig. S17** shows an optical image of a sample spot on a MAMS containing a cluster of several *Chlamydomonas reinhardtii* cells. The image was collected using the white-light microscopy module of an upright NTegra SPECTRA system from NT-MDT (see experimental details, 'Fluorescence and Raman spectroscopy'). The system allows to select specific areas of the sample visible on the optical image for fluorescence and Raman microscopy investigation. Fluorescence and Raman maps of the area marked with the red square were performed using 632.8-nm and 532-nm excitation, respectively. The fluorescence image in **Fig. S17** is based on the emission intensity at the fluorescence maximum at 684 nm and the Raman image shows the intensity distribution of the most prominent β-carotene band at 1520 cm^{-1} after background subtraction. The mapping experiments have confirmed that the green circular structures visible on the optical image are the *C. reinhardtii* cells. At these structures, the Raman signature of β-carotene and the fluorescence emission of chlorophyll were detected. The microspectroscopic maps also demonstrate heterogeneity inside the cell

highlighting pigment-containing organelles. We suppose that such spectroscopic data contains additional information about the cells that is complementary to the metabolite pattern obtained by MALDI-MS and will provide a deeper insight into cell cycle and metabolism of single cells.

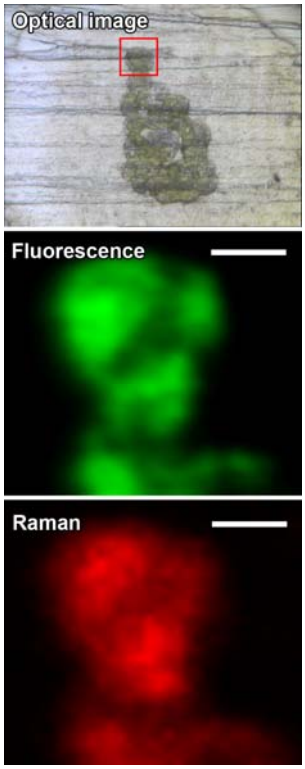

Figure S17. Optical, fluorescence and Raman images of a single cell of *Chlamydomonas reinhardtii*, selected out of several cells present in a 50-µm recipient site of non-transparent MAMS. Scale bar: 5 µm.

Additional references

A. Amantonico, J. Y. Oh, J. Sobek, M. Heinemann and R. Zenobi, *Angew. Chem. Int. Ed.*, 2008, **47**, 5382-5385.

J. L. Edwards and R. T. Kennedy, *Anal. Chem.*, 2005, **77**, 2201-2209.

M. Gilleron, B. Lindner and G. Puzo, *Anal. Chem.*, 2006, **78**, 8543-8548.

Y. Kubo, T. Ikeda, S. Y. Yang and M. Tsuboi, *Appl. Spectrosc.*, 2000, **54**, 1114-1119.

M. L. McLauchlin, D. Yang, P. Aella, A. A. Garcia, S. T. Picraux and M. A. Hayes, *Langmuir*, 2007, **23**, 4871-4877.

S. Saito, M. Tasumi and C. H. Eugster, *J. Raman Spectrosc.*, 1983, **14**, 299-309.

G. Sun, K. Yang, Z. Zhao, S. Guan, X. Han and R. W. Gross, *Anal. Chem.*, 2007, **79**, 6629-6640.

F. Torta, M. Fusi, C. S. Casari, C. E. Bottani and A. Bachi, *J. Proteome Res.*, 2009, **8**, 1932-1942.